

A COSMIC VARIANCE COOKBOOK

BENJAMIN P. MOSTER¹, RACHEL S. SOMERVILLE^{2,3}, JEFFREY A. NEWMAN⁴ AND HANS-WALTER RIX¹

The Astrophysical Journal, submitted

ABSTRACT

Deep pencil beam surveys ($< 1 \text{ deg}^2$) are of fundamental importance for studying the high-redshift universe. However, inferences about galaxy population properties (e.g. the abundance of objects) are in practice limited by ‘cosmic variance’. This is the uncertainty in observational estimates of the number density of galaxies arising from the underlying large-scale density fluctuations. This source of uncertainty can be significant, especially for surveys which cover only small areas and for massive high-redshift galaxies. Cosmic variance for a given galaxy population can be determined using predictions from cold dark matter theory and the galaxy bias. In this paper we provide tools for experiment design and interpretation. For a given survey geometry we present the cosmic variance of dark matter as a function of mean redshift \bar{z} and redshift bin size Δz . Using a halo occupation model to predict galaxy clustering, we derive the galaxy bias as a function of mean redshift for galaxy samples of a given stellar mass range. In the linear regime, the cosmic variance of these galaxy samples is the product of the galaxy bias and the dark matter cosmic variance. We present a simple recipe using a fitting function to compute cosmic variance as a function of the angular dimensions of the field, \bar{z} , Δz and stellar mass m_* . We also provide tabulated values and a software tool. We find that for GOODS at $\bar{z} = 2$ and with $\Delta z = 0.5$ the relative cosmic variance of galaxies with $m_* > 10^{11} M_\odot$ is $\sim 38\%$, while it is $\sim 27\%$ for GEMS and $\sim 12\%$ for COSMOS. For galaxies of $m_* \sim 10^{10} M_\odot$ the relative cosmic variance is $\sim 19\%$ for GOODS, $\sim 13\%$ for GEMS and $\sim 6\%$ for COSMOS. This implies that cosmic variance is a significant source of uncertainty at $\bar{z} = 2$ for small fields and massive galaxies, while for larger fields and intermediate mass galaxies cosmic variance is less serious.

Subject headings: cosmology: theory — galaxies: high-redshift — galaxies: statistics — galaxies: stellar content — large-scale structure of universe

1. INTRODUCTION

Over the last decade, deep ‘pencil beam’ surveys of high-redshift galaxies have been the observational basis for studying the processes that drive galaxy formation and evolution. For a given amount of observing time, such surveys have to trade off imaging area and imaging depth: among HST imaging surveys, GEMS (Rix et al. 2004), AEGIS (Davis et al. 2007) and COSMOS (Scoville et al. 2007) are examples that aim at comparatively wide fields to observe a large sample of galaxies. Alternatively, the Hubble Deep Field (Williams et al. 1996, HDF) and the Ultra Deep Field (Beckwith et al. 2006, UDF) are examples of extremely deep surveys in small areas, aimed at detecting faint galaxies (which can be either of low mass or at high redshift).

One of the most fundamental properties of galaxy sub-populations at any epoch is their number density. However, observational estimates of galaxy number densities in finite volumes are subject to uncertainty due to *cosmic variance*, arising from underlying large-scale density fluctuations and leading to uncertainties in excess of naïve Poisson errors. Note that this source of uncertainty is referred to as ‘sample variance’ in other branches of cosmology. For sampling volumes much larger than the typical clustering scale of the observed objects, cosmic variance is not significant. However,

many important existing surveys have a sampling volume that is small enough that cosmic variance may dominate the uncertainties. This may be particularly true at high redshift, where galaxies are expected to be much more strongly clustered than dark matter (Kauffmann et al. 1999; Baugh et al. 1999; Coil et al. 2004; Moster et al. 2009). Still, many published quantities which are based on number density (e.g. luminosity functions, stellar mass functions, etc.) are quoted with error budgets that do not properly account for cosmic variance. As shown by Trenti & Stiavelli (2008), the normalization and the slope of high-redshift luminosity functions can be affected by cosmic variance errors.

Sound estimates of cosmic variance are helpful both for analyzing existing observational data and for designing future surveys. For a detailed and general treatment of the cosmic error, we refer to Szapudi et al. (1999), Colombi et al. (2000) and Szapudi et al. (2000). Our goal here is to provide a simple recipe to derive cosmic variance for galaxy samples selected by their stellar mass m_* , for a field of specified angular dimensions α_1 and α_2 , at a mean redshift \bar{z} and for a redshift bin size of Δz . Several previous works have provided estimates of cosmic variance for specific sets of assumptions. For example, Newman & Davis (2002) presented estimates of the cosmic variance as a function of field area and axis ratio for the redshift range $0.7 < z < 1.5$, relevant to the DEEP2 redshift survey, but did not account for galaxy bias (the clustering amplitude of galaxies relative to dark matter; see Eqn.13). Somerville et al. (2004) provided predictions that could be used to estimate cosmic variance as a function of mean redshift and survey volume, using the number density of the population to estimate the bias, assuming one galaxy per halo. However, Somerville et al. (2004) used the approximation of

¹ Max-Planck-Institut für Astronomie, Königstuhl 17, 69117 Heidelberg, Germany; moster@mpia.de, rix@mpia.de.

² Space Telescope Science Institute, 3700 San Martin Drive, Baltimore MD 21218; somerville@stsci.edu.

³ Department of Physics and Astronomy, The Johns Hopkins University, 3400 N. Charles St., Baltimore, MD 21218

⁴ Department of Physics and Astronomy, University of Pittsburgh, 3941 O’Hara Street, Pittsburgh, PA 15260; janewman@pitt.edu.

spherical (rather than rectangular or pencil beam) volumes. Trenti & Stiavelli (2008) presented estimates of cosmic variance for pencil beam geometries, again using the number density of the population to estimate the host halo mass and hence the bias.

Many galaxy samples in observational studies, however, are selected by their stellar mass, and stellar mass is one of the fundamental properties of galaxies. Galaxy clustering and bias are strong functions of stellar mass, making it extremely important to account for the mass dependence in cosmic variance estimates. Moreover, one does not necessarily know the number density of a population of interest a priori. We therefore take a different approach here, providing estimates of cosmic variance explicitly as a function of stellar mass and redshift. To do this, we make use of the results previously presented in Moster et al. (2009, M09). We used a Halo Occupation Distribution (HOD) model to empirically establish the relationship between stellar mass and dark matter halo (or sub-halo) mass at different redshifts, and then used a dissipationless N -body simulation to compute the galaxy bias as a function of stellar mass and redshift. We presented fitting functions for this quantity in M09. We combine these with estimates of the cosmic variance for the dark matter for rectangular cells as described in Newman & Davis (2002).

The paper is organized as follows: in Section 2 we describe how to define and how to compute cosmic variance for a galaxy population, based on the underlying cold dark matter (CDM) theory, a model for galaxy bias and for a combination of separate survey fields. In Section 3 we spell out a recipe to compute cosmic variance for a pencil beam geometry in four steps: (1) select survey geometry, (2) choose mean redshift and redshift bin size, (3) determine stellar mass interval and (4) compute cosmic variance. We also apply this recipe to four existing surveys at a redshift of $z = 2$ and $z = 3.5$. In Section 4 we compare cosmic variance for different galaxy samples at different redshifts and different survey geometries. Finally, we summarize our methods and conclusions in Section 5.

Throughout, we assume cosmological parameters consistent with results from WMAP-3 (Spergel et al. 2007) for a flat Λ CDM cosmological model: matter density $\Omega_m = 0.26$, cosmological constant $\Omega_\Lambda = 0.74$, Hubble parameter $H_0 = 72 \text{ km s}^{-1} \text{ Mpc}^{-1}$, fluctuation amplitude $\sigma_8 = 0.77$ and primordial power-spectrum $n_s = 0.95$. All stellar masses are calibrated to a Kroupa (2001) initial mass function.

2. METHOD

The mean $\langle N \rangle$ and the variance $\langle N^2 \rangle - \langle N \rangle^2$ are given by the first and second moments of the probability distribution $P_N(V)$, which describes the probability of counting N objects within a volume V . The relative cosmic variance is defined as

$$\sigma_v^2 = \frac{\langle N^2 \rangle - \langle N \rangle^2 - \langle N \rangle}{\langle N \rangle^2}. \quad (1)$$

The last term in the numerator represents the correction for Poisson shot noise. The second moment of the object counts is

$$\langle N^2 \rangle = \langle N \rangle^2 + \langle N \rangle + \frac{\langle N \rangle^2}{V^2} \int_V dV_a dV_b \xi(|\mathbf{r}_a - \mathbf{r}_b|) \quad (2)$$

where ξ is the two-point correlation function of the sample and V is the sample volume (see Peebles 1980, pg. 234). Combining this with Equation (1), the cosmic variance can

be written as

$$\sigma_v^2 = \frac{1}{V^2} \int_V dV_a dV_b \xi(|\mathbf{r}_a - \mathbf{r}_b|). \quad (3)$$

There are two approaches to evaluating this equation. The first is applicable to populations with a known correlation function, when the integral can be solved either analytically or numerically as a function of cell radius or cell volume. However, in practice, there are a number of difficulties with this approach: while on small scales in the nonlinear regime ($r < 10\text{--}15 \text{ Mpc}$) the correlation function can typically be approximated by a power law, it deviates on larger scales (in the linear regime), from this form. Additionally, in many cases of interest the correlation function is not known a priori.

The second approach to calculating the cosmic variance can be used if the correlation function cannot be approximated by a power law or if it is unknown. It makes use of the galaxy bias, which can be predicted for a given galaxy population using halo occupation models.

We can substitute the galaxy correlation function ξ_{gg} in Equation (3) for the correlation function for dark matter ξ_{dm} :

$$\xi_{gg}(r, m, z) = b^2(m_*, z) \xi_{dm}(r, z), \quad (4)$$

where $b(m_*, z)$ is the galaxy bias, which depends both on redshift z , and the stellar mass of the galaxies m_* . In general, the bias is also a function of r , however, in the linear regime, we assume that it is independent of scale. This assumption will be made throughout the paper. Employing the bias in this manner yields

$$\begin{aligned} \sigma_v^2(m_*, z) &= \frac{1}{V^2} \int_V dV_a dV_b b^2(m_*, z) \xi_{dm}(r_{ab}, z) \\ &= b^2(m_*, z) \frac{1}{V^2} \int_V dV_a dV_b \xi_{dm}(r_{ab}, z) \\ &= b^2(m_*, z) \sigma_{dm}^2(z) \end{aligned} \quad (5)$$

The integral leading to σ_{dm} can then be solved using linear theory in CDM for any volume V with a given geometry. The cosmic variance for galaxies can thus be determined by multiplying the dark matter cosmic variance at a given redshift with the galaxy bias for a given stellar mass at that redshift. For a pencil beam geometry the volume element V is set by the angular size of the survey and the redshift bin size.

We now pursue this second approach, using the galaxy bias as a function of redshift and stellar mass as computed by Moster et al. (2009). In this paper the authors used a halo occupation model to obtain a parameterized stellar-to-halo mass relation by populating halos and subhalos in an N -body simulation with galaxies and requiring that the observed stellar mass function be reproduced. Using the halo positions obtained from the simulation, they find that predictions for the galaxy correlation function are in excellent agreement with observed clustering properties at low redshift. The derived stellar-to-halo mass relation is finally used to predict the stellar-mass-dependent galaxy correlation function and bias at high redshift.

We calculate the cosmic variance for dark matter in each redshift bin by solving the integral in Eqn (3) for dark matter using the code QUICKCV¹ which is described in Newman & Davis (2002). The code computes the dark matter correlation function using the transfer function given in

¹ QUICKCV is available at <http://astro.berkeley.edu/~jnewman/research>

Bardeen et al. (1986) and a window function which is 1 inside the volume V and 0 elsewhere. The volume elements are determined by the angular dimensions of the survey field and the redshift bin. Finally, the cosmic variance for galaxies is computed using Equation (5).

Once cosmic variance has been determined for a number of individual survey fields that are widely separated on the sky, compared to the correlation length, as is often the case (e.g. for the various HST survey fields), one can easily derive the cosmic variance for the combined sample. For the combination of fields i the total volume is

$$V_{\text{tot}} = \sum_i V_i, \quad (6)$$

implying a cosmic variance for the total sample of

$$\begin{aligned} \sigma_{\text{tot}}^2 &= \frac{1}{V_{\text{tot}}^2} \int_V dV_a dV_b \xi(|\mathbf{r}_a - \mathbf{r}_b|) \\ &= \frac{1}{(\sum_i V_i)^2} \int_V d(\sum_i V_i)_a d(\sum_j V_j)_b \xi(|\mathbf{r}_{ia} - \mathbf{r}_{jb}|) \\ &= \frac{1}{(\sum_i V_i)^2} \sum_{ij} \int_V dV_{ia} dV_{jb} \xi(|\mathbf{r}_{ia} - \mathbf{r}_{jb}|) \\ &= \frac{1}{(\sum_i V_i)^2} \sum_i \int_V dV_{ia} dV_{ib} \xi(|\mathbf{r}_{ia} - \mathbf{r}_{ib}|) \\ &= \frac{\sum_i V_i^2 \sigma_i^2}{(\sum_i V_i)^2}. \end{aligned} \quad (7)$$

where we have used

$$\xi(|\mathbf{r}_{ia} - \mathbf{r}_{jb}|) = 0 \text{ for } i \neq j \quad (8)$$

since the galaxies in separated fields are uncorrelated. For a pencil beam geometry (angular extend $\ll 1$ radian) this can be written as

$$\sigma_{\text{tot}}^2 = \frac{\sum_i (\alpha_1 \alpha_2)_i^2 \sigma_i^2}{[\sum_i (\alpha_1 \alpha_2)_i]^2} \quad (9)$$

where α_1 and α_2 are the angular dimensions of each field. Note that this volume-weighted average is identical to an inverse-variance-weighted average only in the range where the cosmic variance scales with volume.

3. RECIPE FOR COSMIC VARIANCE

In order to compute the cosmic variance for galaxies in a given volume in the universe one has to fix five parameters. The size of the volume is determined by two dimensions tangential to the line of sight and one dimension parallel to the line of sight. The tangential dimensions we use are the angular size of the field α_1 and α_2 , while the vertical dimension is set by the size of the redshift bin under consideration Δz . The fourth parameter is the mean redshift of the volume \bar{z} , since the cosmic variance depends on the clustering strength which is a function of redshift. Moreover \bar{z} determines the length scale of the volume bins by setting the conversion factor from angular dimensions and Δz into comoving Mpc. In order to determine the cosmic variance for galaxies one finally has to fix the stellar mass m_* of the sample under consideration, as the clustering strength and the bias depend strongly on stellar mass. Thus the five parameters which have to be set are α_1 , α_2 , \bar{z} , Δz and m_* .

3.1. Survey Geometry

The first step to calculate the cosmic variance is to fix the size of the volume element under consideration. For now

Table 1
Summary of the survey geometries

Survey	N_{field}	α_1^a	α_2^a	area _{field} ^b	total area ^b
UDF	1	3.3	3.3	11	11
GOODS	2	10	16	160	320
GEMS	1	28	28	784	784
EGS	1	10	70	700	700
COSMOS	1	84	84	7056	7056

^a Angular dimension in arcmin

^b Areas in arcmin²

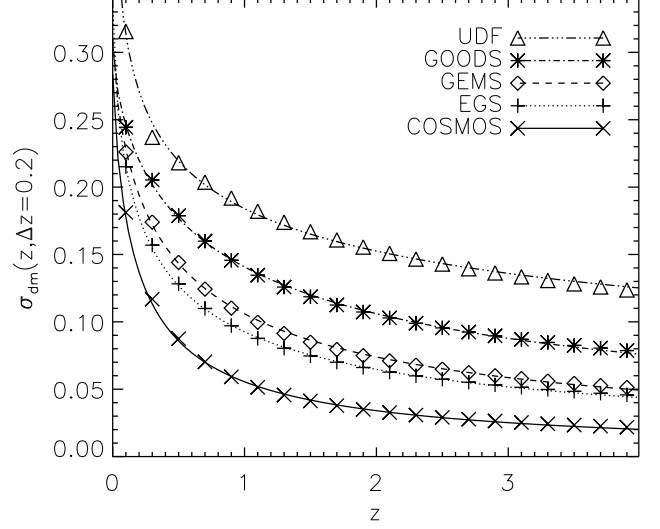


Figure 1. Cosmic variance as a function of mean redshift with a reference bin size of $\Delta z_{\text{ref}} = 0.2$. The different symbols correspond to different fields while the lines are fits to the symbols using Equation (10).

we set the size of the redshift bin to a reference value of $\Delta z = 0.2$. This is a convenient bin size for low redshift while for higher redshift it is rather small. However, this choice can be changed at any redshift (for values $\Delta z \geq 0.05$) using the recipe presented in section 3.2. For the tangential dimensions, we choose five popular fields: the Hubble Ultra Deep Field (Beckwith et al. 2006, UDF), one field of the Great Observatories Origins Deep Survey (Giavalisco et al. 2004, GOODS), the Extended Chandra Deep Field South (E-CDFS) used in the Galaxy Evolution From Morphology And SEDs survey (Rix et al. 2004, GEMS), the Extended Groth Strip (EGS) used in the All-wavelength Extended Groth strip International Survey (Davis et al. 2007, AEGIS) and the field used in the Cosmic Evolution Survey (Scoville et al. 2007, COSMOS). The angular dimensions of the surveys and the resulting observation areas are summarized in Table 1. We note that due to the small scales for the UDF numerical uncertainties in the integration of the correlation function are likely to be high. As a result the values for cosmic variance in the UDF computed here, especially for $z < 0.5$ (where size of the volume elements is very small) have considerable uncertainties. At these scales, the assumption of linear biasing is also not accurate. As a consequence the cosmic variance for the UDF presented here is to be treated with caution and is mainly included to demonstrate the large cosmic variance in small fields.

Table 2

Cosmic variance for different surveys with common redshift bins. The first and second columns show the mean redshift and the redshift bin size, the third column gives the root cosmic variance for dark matter while the last six columns give the root cosmic variance for galaxies in the indicated stellar mass intervals.

\bar{z}	Δz	σ_{dm}	σ_{gg} for $\log(m_*/M_\odot) \pm 0.25$					
			8.75	9.25	9.75	10.25	10.75	11.25
UDF 3.3' \times 3.3'								
0.1	0.2	0.316	0.349	0.358	0.380	0.409	0.430	0.526
0.3	0.2	0.237	0.272	0.288	0.295	0.318	0.339	0.428
0.5	0.2	0.218	0.262	0.273	0.283	0.307	0.332	0.435
0.7	0.2	0.204	0.259	0.271	0.280	0.305	0.335	0.456
0.9	0.2	0.192	0.259	0.274	0.282	0.308	0.346	0.488
1.1	0.2	0.182	0.264	0.281	0.289	0.317	0.365	0.531
1.5	0.2	0.167	0.282	0.305	0.319	0.352	0.426	0.648
1.9	0.2	0.156	0.311	0.341	0.369	0.407	0.518	0.807
2.5	0.2	0.143	0.374	0.416	0.482	0.529	0.718	1.129
3.5	0.2	0.128	0.523	0.593	0.781	0.845	1.236	1.898
GOODS 10' \times 16'								
0.1	0.2	0.244	0.270	0.277	0.294	0.317	0.333	0.407
0.3	0.2	0.205	0.236	0.243	0.255	0.276	0.293	0.371
0.5	0.2	0.179	0.215	0.224	0.232	0.252	0.272	0.357
0.7	0.2	0.160	0.203	0.213	0.220	0.239	0.263	0.358
0.9	0.2	0.146	0.197	0.208	0.214	0.234	0.263	0.371
1.1	0.2	0.135	0.195	0.207	0.214	0.235	0.270	0.392
1.5	0.2	0.119	0.200	0.217	0.227	0.250	0.303	0.460
1.9	0.2	0.107	0.215	0.235	0.255	0.281	0.357	0.557
2.5	0.2	0.096	0.250	0.278	0.322	0.354	0.480	0.754
3.5	0.2	0.083	0.336	0.382	0.503	0.544	0.795	1.221
GEMS 28' \times 28'								
0.1	0.2	0.226	0.250	0.256	0.272	0.293	0.308	0.377
0.3	0.2	0.174	0.200	0.206	0.216	0.234	0.249	0.315
0.5	0.2	0.144	0.173	0.180	0.187	0.203	0.219	0.288
0.7	0.2	0.124	0.158	0.165	0.171	0.186	0.204	0.279
0.9	0.2	0.110	0.149	0.157	0.162	0.177	0.199	0.280
1.1	0.2	0.100	0.144	0.154	0.158	0.174	0.200	0.291
1.5	0.2	0.085	0.143	0.155	0.162	0.179	0.217	0.329
1.9	0.2	0.075	0.150	0.164	0.178	0.196	0.250	0.389
2.5	0.2	0.065	0.170	0.189	0.219	0.240	0.326	0.512
3.5	0.2	0.054	0.221	0.251	0.331	0.358	0.523	0.804
EGS 10' \times 70'								
0.1	0.2	0.215	0.238	0.244	0.259	0.279	0.293	0.358
0.3	0.2	0.157	0.180	0.186	0.195	0.211	0.224	0.284
0.5	0.2	0.128	0.154	0.160	0.167	0.181	0.195	0.256
0.7	0.2	0.120	0.140	0.146	0.151	0.164	0.181	0.246
0.9	0.2	0.097	0.131	0.139	0.143	0.156	0.175	0.247
1.1	0.2	0.088	0.127	0.135	0.139	0.153	0.176	0.256
1.5	0.2	0.075	0.126	0.136	0.143	0.157	0.191	0.290
1.9	0.2	0.066	0.132	0.145	0.157	0.173	0.220	0.343
2.5	0.2	0.057	0.150	0.167	0.194	0.213	0.288	0.453
3.5	0.2	0.048	0.197	0.224	0.295	0.319	0.466	0.716
COSMOS 84' \times 84'								
0.1	0.2	0.181	0.200	0.205	0.218	0.235	0.247	0.302
0.3	0.2	0.117	0.134	0.138	0.145	0.157	0.167	0.211
0.5	0.2	0.088	0.105	0.109	0.114	0.123	0.133	0.175
0.7	0.2	0.070	0.089	0.094	0.097	0.105	0.116	0.158
0.9	0.2	0.059	0.080	0.084	0.087	0.095	0.107	0.151
1.1	0.2	0.051	0.074	0.079	0.083	0.090	0.103	0.150
1.5	0.2	0.041	0.070	0.075	0.079	0.087	0.105	0.160
1.9	0.2	0.035	0.070	0.077	0.083	0.092	0.117	0.182
2.5	0.2	0.029	0.076	0.085	0.098	0.108	0.146	0.230
3.5	0.2	0.023	0.095	0.108	0.142	0.154	0.225	0.346

Table 3

Fitting parameters for different surveys

Survey	σ_a	σ_b	β
UDF	0.251	0.364	0.358
GOODS	0.261	0.854	0.684
GEMS	0.161	0.520	0.729
EGS	0.128	0.383	0.673
COSMOS	0.069	0.234	0.834

3.2. Redshift bins

The next step is to calculate the cosmic variance for dark matter for a set of mean redshifts \bar{z} . We do this using the angular dimensions of the five surveys presented in section 3.1 and the reference redshift bin size of $\Delta z = 0.2$. The cosmic variance is then computed for a set of mean redshifts. The resulting values of the root cosmic variance for dark matter are given in the third column of Table 2 and are plotted in Figure 1 (symbols). To make it possible to obtain the cosmic variance for mean redshifts other than these tabulated values, we introduce a fitting function:

$$\sigma_{dm}(\bar{z}, \Delta z = 0.2) = \frac{\sigma_a}{\bar{z}^\beta + \sigma_b} \quad (10)$$

The parameters σ_a , σ_b and β depend on the angular dimensions of the field and are given in Table 3. The lines in Figure 1 show the fitting function for the five surveys and agree very well with the computed values for the redshift bins. Using Equation (10) for any field we are thus able to calculate the dark matter cosmic variance as a function of mean redshift.

Up until now we have assumed a reference redshift bin size of $\Delta z_{ref} = 0.2$ in order to determine the size of the volume element under consideration. However, especially at higher redshift, larger bin sizes are desirable. We thus investigate how the cosmic variance depends on Δz . For this we plot $\sigma_{dm}(\Delta z)/\sigma_{dm}(\Delta z_{ref})$ as a function of $\Delta z/\Delta z_{ref}$ for different fields and mean redshifts in Figure 2. We find that independent of angular dimensions and mean redshift the cosmic variance has the same dependence on the redshift bin size:

$$\frac{\sigma_{dm}(\Delta z)}{\sigma_{dm}(\Delta z_{ref})} = \left(\frac{\Delta z}{\Delta z_{ref}} \right)^{-0.5} \quad (11)$$

This means that for a reference redshift bin size of $\Delta z_{ref} = 0.2$ as assumed in Equation (10) the root cosmic variance can be calculated for a different Δz as:

$$\sigma_{dm}(\Delta z, \bar{z}) = \sigma_{dm}(\Delta z = 0.2, \bar{z}) \sqrt{\frac{0.2}{\Delta z}} \quad (12)$$

There is a simple picture that explains the dependence on Δz . If we divide a redshift bin of size Δz into N redshift bins with size Δz_i then $\Delta z = N\Delta z_i$. Assuming that all these redshift bins are uncorrelated, we can invoke Equation (9) which yields $\sigma(\Delta z) = \sigma(\Delta z_i)/\sqrt{N}$. Using $N = \Delta z/\Delta z_i$ we finally get $\sigma(\Delta z) = \sigma(\Delta z_i) \times \sqrt{\Delta z_i/\Delta z}$. It is interesting that the simplified assumption of uncorrelated volume elements yields a relation that fits so well to the results calculated for the total redshift bin, as seen in Figure 2. However, we note that this approximation is only valid for redshift bin sizes $\Delta z > 0.05$. For smaller bin sizes we refer to the more accurate model presented in section 3.5 of Newman (2008).

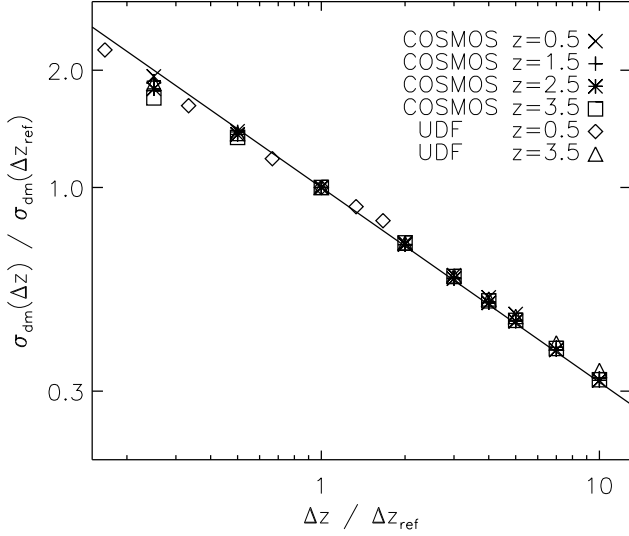


Figure 2. Cosmic variance for different redshift bin sizes normalized to the reference size $\Delta z_{ref} = 0.2$. The different symbols correspond to different fields and mean redshifts and the solid line to $\sqrt{\Delta z_{ref}/\Delta z}$. The dependence on Δz is similar for all geometries and redshifts.

Table 4
Galaxy bias fit parameters

$\log m_g$	b_0	b_1	b_2
8.5 - 9.0	0.062 ± 0.017	2.59 ± 0.18	1.025 ± 0.062
9.0 - 9.5	0.074 ± 0.008	2.58 ± 0.26	1.039 ± 0.028
9.5 - 10.0	0.042 ± 0.003	3.17 ± 0.05	1.147 ± 0.021
10.0 - 10.5	0.053 ± 0.014	3.07 ± 0.17	1.225 ± 0.077
10.5 - 11.0	0.069 ± 0.014	3.19 ± 0.13	1.269 ± 0.087
11.0 - 11.5	0.173 ± 0.035	2.89 ± 0.20	1.438 ± 0.061
> 8.5	0.063 ± 0.008	2.62 ± 0.08	1.104 ± 0.028
> 9.0	0.085 ± 0.008	2.50 ± 0.06	1.098 ± 0.064
> 9.5	0.058 ± 0.005	2.96 ± 0.06	1.192 ± 0.021
> 10.0	0.072 ± 0.013	2.90 ± 0.13	1.257 ± 0.051
> 10.5	0.093 ± 0.015	3.02 ± 0.11	1.332 ± 0.054
> 11.0	0.185 ± 0.032	2.86 ± 0.25	1.448 ± 0.098

Note. — All quoted masses are in units of M_\odot

3.3. Stellar mass dependence

The last step to derive the cosmic variance for a given sample of galaxies is to apply the galaxy bias. As we have shown in Equation (5), in the linear-biasing limit, the cosmic variance for a sample of galaxies with a given stellar mass is the product of the squared bias and the dark matter cosmic variance. The stellar mass dependent galaxy bias has been derived in Moster et al. (2009). The authors present the redshift dependence of the bias using parameterized functions of the form:

$$b(m_*, \bar{z}) = b_0(\bar{z} + 1)^{b_1} + b_2 \quad (13)$$

with the parameters b_0 , b_1 , and b_2 which are given in Table 4 for six stellar mass bins and six stellar mass thresholds. In order to compute the root cosmic variance for galaxies of that mass, we have to multiply the bias and the root cosmic variance of dark matter for the same redshift. This has been done for the five surveys presented in Table 2: the cosmic variance for galaxies of mass m_* is given in columns 4-9 for the reference redshift bin size of $\Delta z = 0.2$. Cosmic variance for massive galaxies is always larger than that of low mass galaxies, since the galaxy bias increases with increasing stellar mass.

3.4. Cookbook for Cosmic Variance

Finally we can summarize our recipe to derive the cosmic variance for a particular survey:

Step 1): Choose the survey (field) in Table 1 that is closest to the field you are using.

Step 2): Choose a mean redshift \bar{z} and a redshift bin size Δz .

Step 3): Choose the stellar mass range of your galaxy sample from Table 4.

Step 4a): Calculate the dark matter root cosmic variance $\sigma_{dm}(\bar{z}, \Delta z = 0.2)$ using Equation (10) and the parameters for your survey as given in Table 3.

Step 4b): Calculate the galaxy bias $b(m_*, \bar{z})$ using Equation (13) and the parameters for your stellar mass bin or threshold as given in Table 4.

Step 4c): Compute the root cosmic variance for galaxies:

$$\sigma_{gg}(m_*, \bar{z}, \Delta z) = b(m_*, \bar{z}) \sigma_{dm}(\bar{z}, \Delta z = 0.2) \sqrt{\frac{0.2}{\Delta z}}$$

Step 4d): Combine widely separated fields using Equation (9).

This recipe allows for easy computation of cosmic variance for the representative surveys we have presented. To enable readers to compute cosmic variance for different survey areas or geometries, we provide a software tool as an online supplement². For specified angular dimensions and redshift bins the code computes the cosmic variance for dark matter and galaxies in six stellar mass bins.

3.5. Examples

Having derived the recipe to determine the cosmic variance, we can apply it to the five example surveys. We first give an overview of the surveys. The UDF is an exposure of a square field in the southern sky covering a total area of 11 arcmin² with the Advanced Camera for Surveys (ACS) on the Hubble Space Telescope (HST). To date it is the deepest image of the universe with uniform limiting magnitudes $m \sim 29$ for point sources and contains at least 10,000 objects. However, of the five surveys studied here, the UDF is the smallest. The GOODS project covers two fields, the Hubble Deep Field North (HDFN) and the Chandra Deep Field South (CDFN) which both have similar dimensions of $\approx 10 \times 16$ arcmin² and are so widely separated as to be uncorrelated. Since for widely separated fields the cosmic variance goes as $1/N_{\text{field}}$, the total variance for both fields decreases by a factor of 2. The GEMS survey has imaged the E-CDFN, a square area of 784 arcmin², with the ACS on the HST. The E-CDFN is centered on the CDFN and contains roughly 10,000 galaxies down to a depth of 24th magnitude in the R-band. AEGIS is a multi-wavelength, deep, wide-field, photometric and spectroscopic survey in the Extended Groth Strip (EGS) area. While the total area is similar to that of GEMS, the field is a long strip with dimensions of $\approx 10 \times 70$ arcmin². The widest survey for which we compute cosmic variance is COSMOS which covers an equatorial square field of 2 deg² with

² IDL code available at <http://www.mpia.de/homes/moster/research>

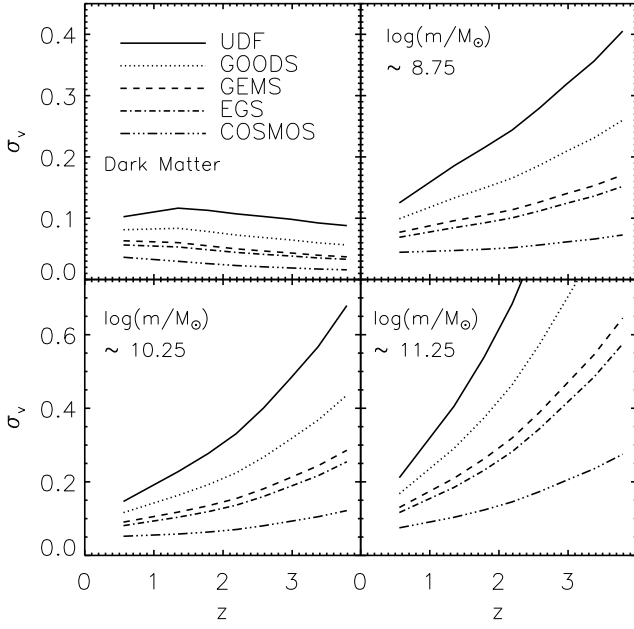


Figure 3. The root cosmic variance as a function of redshift with redshift bins of constant volume. The four panels are for dark matter and galaxies in three stellar mass bins. The lines are for different surveys.

imaging by most of the major space-based telescopes and several large ground-based telescopes. The magnitude limit in the I-band is $I \sim 27$.

If we apply this recipe to the UDF, GOODS, GEMS, AEGIS and COSMOS at $\bar{z} = 2$ and $\Delta z = 0.5$, the relative cosmic variance for massive galaxies with $m_* > 10^{11} M_\odot$ is $\sim 55\%$ for the UDF, while it is $\sim 38\%$ for GOODS, $\sim 27\%$ for GEMS, $\sim 23\%$ for AEGIS and $\sim 12\%$ for COSMOS. For galaxies of intermediate mass ($m_* \sim 10^{10} M_\odot$) the relative cosmic variance is $\sim 27\%$ for the UDF, $\sim 19\%$ for GOODS, $\sim 13\%$ for GEMS, $\sim 11\%$ for AEGIS and $\sim 6\%$ for COSMOS. This implies that at $\bar{z} = 2$ cosmic variance is a significant source of uncertainty for small fields and massive galaxies. However, for larger fields and intermediate mass galaxies cosmic variance is less serious.

At a higher redshift of $\bar{z} = 3.5$ and $\Delta z = 0.5$ the relative cosmic variance is higher, since the galaxy bias is much larger. For massive galaxies with $m_* > 10^{11} M_\odot$, we find a relative cosmic variance of $\sim 124\%$ for the UDF, $\sim 78\%$ for GOODS, $\sim 51\%$ for GEMS, $\sim 45\%$ for AEGIS and $\sim 21\%$ for COSMOS. For intermediate mass galaxies with $m_* \sim 10^{10} M_\odot$ the relative cosmic variance is $\sim 54\%$ for the UDF, $\sim 34\%$ for GOODS, $\sim 22\%$ for GEMS, $\sim 20\%$ for AEGIS and $\sim 9\%$ for COSMOS. This shows that at $\bar{z} = 3.5$ cosmic variance can be serious in small fields even for intermediate mass galaxies. For massive galaxies even the widest survey (COSMOS) has considerable uncertainties due to cosmic variance.

4. SCALING OF COSMIC VARIANCE

It is not very useful to compare the cosmic variance at different redshifts for a fixed bin size, because the volumes are not the same. Since cosmic variance strongly depends on the volume of the sample under consideration, we choose redshift bins such that all redshift bins have the same volume. This allows us to directly compare the cosmic variance at different redshifts. The results of this analysis are given in Table 5 for the GOODS, GEMS and COSMOS surveys.

Table 5

Cosmic variance for different surveys with constant comoving volume. The first and second columns show the mean redshift and the redshift bin size, the third column gives the root cosmic variance for dark matter, and the last six columns give the root cosmic variance for galaxies in the indicated stellar mass intervals.

z_{\min}	z_{\max}	σ_{dm}	σ_{gg} for $\log(m_*/M_\odot) \pm 0.25$					
			8.75	9.25	9.75	10.25	10.75	11.25
GOODS $10' \times 16'$								
0.00	1.12	0.081	0.099	0.103	0.107	0.116	0.126	0.168
1.12	1.58	0.084	0.133	0.143	0.148	0.163	0.194	0.291
1.58	1.99	0.078	0.149	0.163	0.174	0.192	0.241	0.374
1.99	2.39	0.073	0.165	0.183	0.204	0.225	0.295	0.464
2.39	2.78	0.069	0.186	0.208	0.243	0.267	0.365	0.573
2.78	3.17	0.065	0.209	0.235	0.290	0.316	0.446	0.696
3.17	3.58	0.060	0.231	0.262	0.339	0.368	0.534	0.823
3.58	4.00	0.056	0.260	0.296	0.404	0.436	0.647	0.983
GEMS $28' \times 28'$								
0.00	1.12	0.063	0.077	0.080	0.083	0.091	0.098	0.130
1.12	1.58	0.060	0.096	0.103	0.107	0.118	0.140	0.210
1.58	1.99	0.055	0.105	0.114	0.122	0.135	0.169	0.262
1.99	2.39	0.050	0.114	0.126	0.140	0.155	0.203	0.319
2.39	2.78	0.047	0.126	0.141	0.165	0.181	0.247	0.389
2.78	3.17	0.043	0.140	0.158	0.194	0.212	0.299	0.466
3.17	3.58	0.040	0.153	0.173	0.225	0.244	0.354	0.545
3.58	4.00	0.037	0.171	0.194	0.265	0.286	0.425	0.645
COSMOS $84' \times 84'$								
0.00	1.12	0.036	0.044	0.046	0.048	0.052	0.057	0.075
1.12	1.58	0.030	0.047	0.051	0.053	0.058	0.069	0.104
1.58	1.99	0.026	0.049	0.054	0.058	0.064	0.080	0.124
1.99	2.39	0.023	0.052	0.057	0.064	0.070	0.093	0.145
2.39	2.78	0.021	0.056	0.063	0.074	0.081	0.110	0.173
2.78	3.17	0.019	0.061	0.069	0.085	0.093	0.131	0.204
3.17	3.58	0.017	0.066	0.075	0.097	0.105	0.153	0.235
3.58	4.00	0.016	0.073	0.083	0.113	0.122	0.181	0.275

4.1. Cosmic variance for different redshifts

We would expect the cosmic variance of dark matter to decrease monotonically with increasing redshift, because it depends on the clustering which is lower for high redshift. However, we see, that for the UDF σ_{dm} increases, reaches a maximum and then decreases with increasing redshift, while for the other surveys σ_{dm} decreases with increasing redshift. The reason for this is that although the different redshift bins have the same comoving volume, their geometry is not the same. This is due to the pencil beam geometry for which the volume of the low redshift bins are long but narrow, while the higher redshift bins become shorter and wider. Thus with increasing redshift the ratio of the area and the depth of the redshift bins increases. In the lower redshift bins the galaxies are thus on average more separated than in the higher redshift bins. This causes the cosmic variance to increase with redshift. At high redshift and for very wide surveys the ratio decreases again with redshift as the line of sight distance in a redshift bin becomes smaller than the transverse distance.

Both effects, the decrease of σ_{dm} with redshift due to lower clustering amplitudes and the growth of σ_{dm} because of the geometry of the redshift bins, affect $\sigma_{dm}(z)$. The redshift at which σ_{dm} is maximal depends on the area of the survey. For small areas (e.g. UDF) it is higher ($z_{\max} \sim 1.3$) while for large

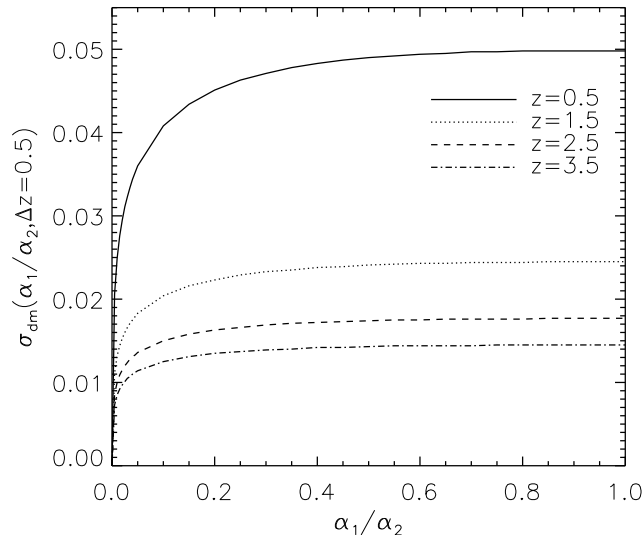


Figure 4. Effects of survey geometry on cosmic variance. The root cosmic variance of dark matter is plotted as a function of the ratio between the two observation angles α_1/α_2 . The lines represent different redshift bins with a bin size of $\Delta z = 1.0$.

areas (e.g. COSMOS) it is lower ($z_{max} < 0.2$). The cosmic variance for the galaxy samples we consider, however, always increases with redshift. This is due to the large biases of these samples, which are always larger than unity. Since the bias increases strongly with redshift, the cosmic variance for galaxies thus also increases with redshift.

Figure 3 plots the cosmic variance as a function of redshift with redshift bins of constant volume. The four different panels show σ_v for dark matter and three stellar mass bins. The lines are for different surveys. We see that except for the UDF, the cosmic variance for dark matter decreases with redshift while for all surveys the cosmic variance for galaxies increases with redshift.

4.2. Cosmic variance for different geometries

As we have shown, cosmic variance depends strongly on the geometry of the survey. In section 4.1 we investigated the geometric effect that arises because of the ratio between line-of-sight distance and the transverse distance in the redshift bins. Now we investigate the effects that arise due to different angular geometry on the sky. For this we assume a survey with a fixed total area of 1.0 deg^2 . We vary the ratio between the two observation angles α_1/α_2 from $\alpha_1/\alpha_2 \approx 0$ to $\alpha_1/\alpha_2 = 1$. This is done for several mean redshifts with a bin size of $\Delta z = 0.5$.

Figure 4 shows the geometry effects on the cosmic variance. It plots σ_{dm} as a function of the ratio between the two observation angles. The result agrees with our explanation in section 4.1: for a low ratio the cosmic variance is very low. If one increases the ratio the cosmic variance quickly increases and reaches its maximum at $\alpha_1/\alpha_2 = 1$. Here the mean distance between the observed galaxies is the smallest, so that many galaxies are likely to be correlated, resulting in large cosmic variance.

This effect can also be seen by comparing the cosmic variance for GEMS and EGS at a fixed redshift bin. We find that although the area of the GEMS field is larger than that of the EGS, GEMS has a higher cosmic variance. However, we note that unless the ratio between the observation angles is smaller than $\sim 20\%$, this effect is small. In agreement with Newman & Davis (2002), we find that the size of the survey

area is much more important than the axis ratio.

5. CONCLUSIONS

Inferences about galaxy number densities and related quantities such as luminosity and stellar mass functions are subject to uncertainties due to cosmic variance. It can be a significant source of uncertainty, especially for surveys which cover only small areas and for massive high-redshift galaxies. We have derived a simple recipe to compute cosmic variance for five surveys as a function of mean redshift \bar{z} , redshift bin size Δz and the stellar mass of the galaxy population m_* .

For this recipe we first calculated the dark matter cosmic variance as a function of mean redshift and for a reference bin size of $\Delta z_{red} = 0.2$. This was done by integrating the dark matter correlation function obtained from CDM theory for a pencil beam geometry in a redshift bin. We provide fitting functions for five surveys (UDF, GOODS, GEMS, AEGIS, COSMOS). We then showed that the dependence of cosmic variance on bin size Δz is nearly independent of mean redshift and survey geometry. This means that cosmic variance for a different bin size can be estimated from the value computed with the reference bin size using a simple conversion factor. We have used the galaxy bias predictions by Moster et al. (2009) (for six stellar mass bins and six thresholds) and the dark matter cosmic variance to compute the cosmic variance for galaxies. We also presented a formula to compute the overall cosmic variance for a volume-weighted average of multiple separated fields.

Applying this recipe to GOODS, GEMS and COSMOS at $\bar{z} = 2$ and $\Delta z = 0.5$, the relative cosmic variance for galaxies with $m_* > 10^{11} M_\odot$ ($m_* \sim 10^{10} M_\odot$) is $\sim 38\%$ (19%) for GOODS, while it is $\sim 27\%$ (13%) for GEMS and $\sim 12\%$ (6%) for COSMOS. At $\bar{z} = 3.5$ and $\Delta z = 0.5$ we found a relative cosmic variance for galaxies with $m_* > 10^{11} M_\odot$ ($m_* \sim 10^{10} M_\odot$) of $\sim 78\%$ (34%) for GOODS, $\sim 51\%$ (22%) for GEMS and $\sim 21\%$ (9%) for COSMOS.

We find that for all fields the cosmic variance is much more significant for massive galaxies, which is due to the strong dependence of the galaxy bias on stellar mass. Our results imply that cosmic variance is a significant source of uncertainty at $\bar{z} = 2$ for small fields and massive galaxies, while for larger fields and intermediate mass galaxies, cosmic variance is less serious. At $\bar{z} = 3.5$ cosmic variance can become serious in small fields even for intermediate mass galaxies. For massive galaxies even the widest survey (COSMOS) has significant uncertainties due to cosmic variance.

BPM thanks the Space Telescope Science Institute for hospitality during part of this work. JAN acknowledges support from NSF grant AST-0806732.

REFERENCES

- Bardeen, J. M., Bond, J. R., Kaiser, N., & Szalay, A. S. 1986, ApJ, 304, 15
- Baugh, C. M., Benson, A. J., Cole, S., Frenk, C. S., & Lacey, C. G. 1999, MNRAS, 305, L21
- Beckwith, S. V. W., et al. 2006, AJ, 132, 1729
- Coil, A. L., et al. 2004, ApJ, 609, 525
- Colombi, S., Szapudi, I., Jenkins, A., & Colberg, J. 2000, MNRAS, 313, 711
- Davis, M., et al. 2007, ApJ, 660, L1
- Giavalisco, M., et al. 2004, ApJ, 600, L93
- Kauffmann, G., Colberg, J. M., Diaferio, A., & White, S. D. M. 1999, MNRAS, 307, 529
- Kroupa, P. 2001, MNRAS, 322, 231
- Newman, J. A., & Davis, M. 2002, ApJ, 564, 567

- Newman, J. A. 2008, *ApJ*, 684, 88
- Moster, B. P., Somerville, R. S., Maulbetsch, C., van den Bosch, F. C., Maccio', A. V., Naab, T., & Oser, L. 2009, arXiv:0903.4682
- Peebles, P. J. E. 1980, *The Large-Scale Structure of the Universe* (Princeton: Princeton University Press)
- Rix, H.-W., et al. 2004, *ApJS*, 152, 163
- Scoville, N., et al. 2007, *ApJS*, 172, 1
- Somerville, R. S., Lee, K., Ferguson, H. C., Gardner, J. P., Moustakas, L. A., & Giavalisco, M. 2004, *ApJ*, 600, L171
- Spergel, D. N., et al. 2007, *ApJS*, 170, 377
- Szapudi, I., Colombi, S., & Bernardeau, F. 1999, *MNRAS*, 310, 428
- Szapudi, I., Colombi, S., Jenkins, A., & Colberg, J. 2000, *MNRAS*, 313, 725
- Trenti, M., & Stiavelli, M. 2008, *ApJ*, 676, 767
- Williams, R. E., et al. 1996, *AJ*, 112, 1335